



# Population Pharmacokinetics of an Anti-PD-L1 Antibody, Durvalumab in Patients with Hematologic Malignancies

Ken Ogasawara<sup>1</sup> · Kathryn Newhall<sup>2</sup> · Stephen E. Maxwell<sup>1</sup> · Justine Dell'Aringa<sup>2</sup> · Vitalina Komashko<sup>2</sup> · Nurgul Kilavuz<sup>1</sup> · Richard Delarue<sup>3</sup> · Myron Czuczman<sup>1</sup> · Lars Sternas<sup>1</sup> · Shelonitda Rose<sup>1</sup> · C. L. Beach<sup>4</sup> · Steven Novick<sup>1</sup> · Simon Zhou<sup>1</sup> · Maria Palmisano<sup>1</sup> · Yan Li<sup>1</sup>

Published online: 22 July 2019  
© The Author(s) 2019

## Abstract

**Background and Objectives** Durvalumab, a human monoclonal antibody targeting programmed cell death ligand 1, has been approved for urothelial carcinoma and stage III non-small cell lung cancer by the US Food and Drug Administration and is being evaluated in various malignancies. The objective of this study was to develop a population-pharmacokinetic model of durvalumab in patients with various hematologic malignancies and to investigate the effects of demographic and disease factors on the pharmacokinetics in this population.

**Methods** A total of 1812 concentrations from 267 patients with myelodysplastic syndromes, acute myeloid leukemia, multiple myeloma, non-Hodgkin lymphoma, or Hodgkin lymphoma were included in the analysis.

**Results** The pharmacokinetics of durvalumab was adequately described by a two-compartment model with first-order elimination. A decrease in durvalumab clearance over time was mainly explained by incorporation of time-dependent changes in albumin (in all patients) and immunoglobulin G (in patients with multiple myeloma) into the model. For multiple myeloma, patients with immunoglobulin G  $\geq 20$  g/L showed a 30% lower area under the concentration–time curve at cycle 1 compared with patients with immunoglobulin G  $< 20$  g/L. The impact of any baseline covariates on durvalumab pharmacokinetics did not appear to be clinically relevant. The pharmacokinetics of durvalumab in hematologic malignancies was generally consistent with previously reported pharmacokinetics in solid tumors.

**Conclusions** These results support the same dosing regimen (1500 mg every 4 weeks) for both solid tumors and hematologic malignancies from the perspective of adequate exposure. Additionally, total immunoglobulin G level could be a critical covariate for the pharmacokinetics of monoclonal antibodies in patients with multiple myeloma.

## 1 Introduction

The programmed cell death 1 (PD-1)/programmed cell death ligand 1 (PD-L1) pathway plays a critical role in maintaining an immunosuppressive tumor

**Electronic supplementary material** The online version of this article (<https://doi.org/10.1007/s40262-019-00804-x>) contains supplementary material, which is available to authorized users.

✉ Yan Li  
yali@celgene.com

- <sup>1</sup> Celgene Corporation, Summit, NJ, USA
- <sup>2</sup> Celgene Corporation, Seattle, WA, USA
- <sup>3</sup> Celgene Corporation, Boudry, Switzerland
- <sup>4</sup> Celgene Corporation, Kansas City, KS, USA

### Key Points

A population-pharmacokinetic model of durvalumab was developed in patients with various hematologic malignancies including myelodysplastic syndromes, acute myeloid leukemia, multiple myeloma, non-Hodgkin lymphoma, or Hodgkin lymphoma

The pharmacokinetics of durvalumab in hematologic malignancies was generally consistent with that in solid tumors, and these results support the same dosing regimen (1500 mg every 4 weeks) for both solid tumors and hematologic malignancies from the perspective of adequate exposure

Total immunoglobulin G level could be a critical covariate for the pharmacokinetics of monoclonal antibodies in patients with multiple myeloma

microenvironment and the blockade of PD-1/PD-L1 pathway has become the key component of cancer immunotherapy [1]. Durvalumab (MEDI4736) is a human immunoglobulin G1 (IgG1) kappa monoclonal antibody that binds to PD-L1, blocking the ability to bind to PD-1 or a cluster of differentiation 80 on activated T cells, leading to immune-mediated killing [2]. Durvalumab has been approved for the treatment of patients with urothelial carcinoma and stage III non-small cell lung cancer by the US Food and Drug Administration [3], and is currently being evaluated in various solid tumors and hematologic malignancies, including non-Hodgkin lymphoma (NHL), multiple myeloma (MM), myelodysplastic syndromes (MDS), and acute myeloid leukemia (AML). Anti-PD-1 antibodies (nivolumab and pembrolizumab) and other anti-PD-L1 antibodies (atezolizumab and avelumab) have also been approved for the indication of various solid tumors and some hematologic malignancies such as classical Hodgkin lymphoma and primary mediastinal large B-cell lymphoma [3].

The pharmacokinetics of these PD-1/PD-L1 inhibitors is largely similar to that of endogenous IgG, except the time-varying clearance (CL) [4]. Clearance of PD-1/PD-L1 inhibitors decreases over time, which appears to be associated with response to treatment [4]. Population-pharmacokinetic (PK) models of anti-PD-1/PD-L1 antibodies in solid tumors have been reported [5–11], and the PK profiles of anti-PD-1/PD-L1 antibodies were typically characterized by a two-compartment model with linear elimination [4]. A time-dependent decrease in CL of nivolumab and pembrolizumab was described with empirical time-varying CL models [6, 8, 9]. Baverel et al. [7] recently reported the population-PK analysis of durvalumab in solid tumors, where the change in CL over time was well explained by a semi-mechanistic time-varying CL model with longitudinal covariates related to disease status. For hematologic malignancies, one population-PK model has been reported for nivolumab in patients with classical Hodgkin lymphoma, indicating consistent PK properties with solid tumors except for a lower baseline CL by 28% [12]. However, population-PK analyses of PD-1/PD-L1 inhibitors in other common hematologic malignancies such as NHL and MM have not been reported.

In this study, a population-PK model of durvalumab was developed using pooled data from four clinical trials of hematologic malignancies (NHL, MM, MDS, and AML), and the model structure and covariate effects were compared with those in solid tumors. In addition, differences in durvalumab pharmacokinetics and the covariate effects among hematologic malignancies were explored.

## 2 Methods

### 2.1 Clinical Study Data

Four clinical studies of durvalumab (MEDI4736-MDS-001 [NCT02775903], MEDI4736-MM-002 [NCT02685826], MEDI4736-MM-005 [NCT03000452], and MEDI4736-NHL-001 [NCT02733042]) were included in the population-PK analyses (Table 1). Data available as of September 2018 were used. These studies have been conducted in accordance with the Declaration of Helsinki and the International Council for Harmonisation Guideline for Good Clinical Practice (ICH E6). Written informed consent was obtained from all subjects.

### 2.2 Bioanalytical Methods

Serum durvalumab concentrations were measured using validated electrochemiluminescence method with a lower limit of quantification of 0.050 µg/mL and an upper limit of quantification of 1.600 µg/mL. Soluble PD-L1 (sPD-L1) that is not bound to durvalumab in human serum was measured using a validated electrochemiluminescence immunoassay with a lower limit of detection of 67.1 pg/mL and an upper limit of quantification of 1000 pg/mL.

### 2.3 Population-Pharmacokinetic Analyses

A total of 1812 serum durvalumab concentrations from 267 patients were used in the population-PK analyses. Population-PK models were developed using a nonlinear mixed-effect modeling approach, as implemented in the NONMEM software version 7.3.0 (ICON Development Solutions, Ellcott City, MD, USA). Plotting of NONMEM outputs was conducted using the R software (version 3.4.1) and RStudio (version 1.1.456; Boston, MA, USA).

In the development of the structural PK model, one- to three-compartment models with linear CL and/or nonlinear (Michaelis–Menten) CL and/or empirical time-varying CL were tested to fit serum concentration–time data. An empirical time-varying CL model was described as follows:

$$CL_{t,i} = CL_i \cdot \exp\left(\frac{E_{\max} \cdot t^\gamma}{T_{50}^\gamma + t^\gamma}\right),$$

where  $CL_{t,i}$  represents the CL of subject  $i$  at a given time  $t$ ,  $CL_i$  represents the baseline CL of subject  $i$ ,  $E_{\max}$  represents the maximum change in CL over time,  $T_{50}$  represents the time at which the change is half of its maximum, and  $\gamma$  represents the shape parameter that describes the degree of sigmoidicity. A fixed value of  $\gamma$  was not explored because

**Table 1** Summary of clinical studies used in the population-pharmacokinetic (PopPK) modeling

Study	Dosing regimen	Scheduled PK timepoints	Number of subjects in PopPK	Number of PK samples in PopPK
MEDI4736-MDS-001: A randomized, multicenter, open-label, phase II study evaluating the efficacy and safety of azacitidine subcutaneously in combination with durvalumab (MEDI4736) in previously untreated subjects with higher risk myelodysplastic syndromes, elderly subjects (aged $\geq 65$ years), or subjects with acute myeloid leukemia not eligible for hematopoietic stem cell transplantation	1500 mg, 1-h IV infusion, Q4W	Cycle 1: end of infusion; Cycle 2: pre-infusion; Cycle 4: pre-infusion and end of infusion; Cycle 6: pre-infusion	99	340
MEDI4736-MM-002: A phase I/II, multicenter, open-label study to determine the recommended dose and regimen of durvalumab (MEDI4736) in combination with lenalidomide with and without dexamethasone in subjects with newly diagnosed MM	1500 mg, 1-h IV infusion, Q4W	Cycle 1: pre-infusion, end of infusion, 4, 168, 336, and 504 h post-infusion; Cycle 2: pre-infusion, end of infusion, 4 and 336 h post-infusion; Cycles 4, 6, 10, and 14: pre-infusion	55	503
MEDI4736-MM-005: A multicenter, single-arm, phase II study to determine the efficacy of the combination of daratumumab plus durvalumab (D2) in subjects with relapsed and refractory MM who have progressed on daratumumab while on a daratumumab-containing regimen as the most recent MM therapy	1500 mg, 1-h IV infusion, Q4W	Cycle 1: pre-infusion, end of infusion, 144, 312, and 480 h post-infusion; Cycles 2 and 4: pre-infusion	18	74
MEDI4736-NHL-001: A phase I/II, open label, multicenter study to assess the safety and tolerability of durvalumab (anti-PD-L1 antibody) as monotherapy and in combination therapy in subjects with lymphoma or chronic lymphocytic leukemia	1500 mg, 1-h IV infusion, Q4W	Cycle 1: pre-infusion, end of infusion, 4, 24, 48, 168, 336, and 504 h post-infusion; Cycle 2: pre-infusion, end of infusion, 4 and 336 h post-infusion; Cycles 4, 6, and 10: pre-infusion	95	895

*h* hours, *IV* intravenous, *MEDI4736* durvalumab, *MM* multiple myeloma, *PD-L1* programmed cell death ligand 1, *Q4W* every 4 weeks

the  $\gamma$  value in the population-PK model of durvalumab in solid tumors [7] could be different from that in hematologic malignancies, and  $E_{\max}$  and  $T_{50}$  are sensitive to  $\gamma$ . Serum durvalumab concentrations were log-transformed prior to the analyses. First-order conditional estimation with interaction was used for parameter estimation. The inter-subject variability was modeled assuming a log-normal distribution. Residual variability was modeled using an additive model. The model selection was based on minimum objective function values (OFVs), precision of parameter estimates, condition number, and goodness-of-fit plots. Covariate model building was carried out using a stepwise procedure, with significant levels set to 0.01 and 0.001 for the forward inclusion and backward elimination steps, respectively.

Factors related to demographics (age, sex, body weight, race, and ethnicity), liver function (aspartate aminotransferase, alanine aminotransferase, and total bilirubin), kidney function (creatinine CL), and disease status at baseline (Eastern Cooperative Oncology Group performance status and tumor type) were tested as baseline covariates. Longitudinal markers related to disease status [albumin, IgG, sPD-L1, and lactate dehydrogenase (LDH)] were tested as time-varying covariates. Longitudinal IgG data were available only from MEDI4736-MM-002 and MEDI4736-MM-005, and only baseline IgG levels were included from MEDI4736-NHL-001. Immunoglobulin levels were not available from MEDI4736-MDS-001. Soluble PD-L1 levels below the lower limit of detection was imputed as a lower limit of detection/2 (33.55 pg/mL). Missing baseline covariates were imputed as the median value in the study population. The last observation carried forward method was used to fill in missing values at later points.

The nonparametric bootstrap resampling technique was used to assess the precision of the parameter estimates of the final population-PK model. One thousand bootstrap datasets were created by randomly resampling the original dataset with replacement. The predictability of the final model was evaluated using a visual predictive check, which was constructed using 200 simulated replicates of the original dataset. The nonparametric 90% confidence interval (CI) of the median and the 5th and 95th prediction percentiles of the simulated concentrations at each binned timepoint were visually compared with the median and 5th and 95th percentiles of the observed concentrations.

For the assessment of effects of covariates or type of malignancies on durvalumab exposure, the area under the concentration–time curve of durvalumab at cycle 1 ( $AUC_{C1}$ ) was used as the exposure parameter and calculated based on Bayesian estimates of PK parameters at baseline from the final population-PK model. In addition, the durvalumab PK profile during cycle 1 was simulated at both a fixed dose (1500 mg) and a weight-based dose (20 mg/kg) using 267 patients in the population-PK dataset.

## 3 Results

### 3.1 Demographics

The population-PK dataset included data from 267 subjects with various types of hematologic malignancies. Demographic characteristics of these subjects are shown in Table 2, and generally comparable to those in the population-PK analysis of durvalumab in solid tumors [7].

### 3.2 Base Population-Pharmacokinetic Model of Durvalumab

The pharmacokinetics of durvalumab was adequately described by a two-compartment model with first-order elimination (linear CL). Inter-individual variability was estimated for CL and the volume of distribution of central compartment ( $V_c$ ). Nonlinear (Michaelis–Menten) CL was not included in the base model owing to poor precision of Michaelis–Menten parameter estimates [Michaelis–Menten constant ( $K_m$ ) and maximum elimination rate ( $V_{\max}$ )] and poor stability of the model. Similarly, the empirical time-varying CL model was not implemented in the base model because the time-varying CL parameter ( $\gamma$ ) was estimated with poor precision.

### 3.3 Final Population-Pharmacokinetic Model of Durvalumab

The parameters of the final model, including bootstrap medians and 95% CIs for the PK parameters, are presented in Table 3. The main steps of the covariate model building from the base model to the final model are summarized in Table 1 of the Electronic Supplementary Material (ESM). All covariates added in the forward inclusion step ( $\Delta\text{OFV} < -6.635$ ,  $p < 0.01$ ) were retained in the backward elimination step ( $\Delta\text{OFV} > 10.828$ ,  $p < 0.001$ ). The final population-PK model included the following covariates: albumin (time varying), sex and body weight (baseline) on both CL and  $V_c$ , IgG (time varying), sPD-L1 (time varying), LDH (time varying) and MDS/AML on CL, and MM on  $V_c$ . Adding the time-dependent change in albumin and IgG on CL significantly decreased the OFV by 239 and 153, respectively, while effects of other covariates on the OFV were  $-15$  to  $-35$  (Table 1 of the ESM). Lower albumin level, higher body weight, and male sex were associated with higher CL and  $V_c$  independently, and higher IgG, sPD-L1, and LDH levels were associated with higher CL. Patients with MM had lower  $V_c$  compared with those with non-MM, and patients with MDS/AML had higher CL than those with non-MDS/AML. Figures 1 and 2 present goodness-of-fit plots for the final model and the visual predictive check, respectively. Changes in durvalumab CL with time were

**Table 2** Baseline demographic and disease characteristics of 267 patients with hematologic malignancies

Characteristics				
Continuous variables	Median	(Range)	Missing, <i>N</i> (%)	LOCF, <i>n</i> (%)
Age (years)	71	(21–89)	0 (0)	NA
Weight (kg)	74.7	(37.7–121)	0 (0)	NA
Creatinine clearance (mL/min)	73.9	(8.96–272)	1 (0.4)	NA
Aspartate aminotransferase (U/L)	19	(9–84)	0 (0)	NA
Alanine aminotransferase (U/L)	16	(5–127)	0 (0)	NA
Total bilirubin (μmol/L)	7.7	(2.6–28)	0 (0)	NA
Serum albumin (g/L)	40	(23–50)	0 (0)	568 (31.3)
Lactate dehydrogenase (U/L)	216	(89–1481)	1 (0.4)	644 (35.5)
Soluble PD-L1 (pg/mL)	173.8	(72.0–985)	30 (11.2)	899 (49.6)
Immunoglobulin A (g/L)	0.64	(0.28–53)	100 (37.5)	NA
Immunoglobulin G (g/L)	7.6	(0.70–74)	100 (37.5)	379 (20.9)
Immunoglobulin M (g/L)	0.24	(0.20–11)	100 (37.5)	NA
Categorical variables	<i>N</i>	(%)		
<b>Sex</b>				
Male	173	(64.8)		
Female	94	(35.2)		
<b>Race</b>				
Caucasian	185	(69.3)		
African–American	4	(1.5)		
Asian	16	(6.0)		
Others	6	(2.2)		
Unknown	56	(21.0)		
<b>Ethnicity</b>				
Hispanic or Latino	11	(4.1)		
Non-Hispanic or Latino	198	(74.2)		
Unknown	58	(21.7)		
<b>ECOG</b>				
0	121	(45.3)		
1	120	(44.9)		
2	23	(8.6)		
3	1	(0.4)		
Unknown	2	(0.7)		
<b>Tumor</b>				
NHL	90	(33.7)		
DLBCL	32	(12.0)		
FL	22	(8.2)		
MCL	17	(6.4)		
CLL/SLL	13	(4.9)		
MZL	5	(1.9)		
tFL	1	(0.4)		
MM	73	(27.3)		
AML	61	(22.8)		
MDS	38	(14.2)		
HL	5	(1.9)		
<b>Co-administration</b>				
Monotherapy	26	(9.7)		
Combination therapy	241	(90.3)		

*AML* acute myeloid leukemia, *CLL* chronic lymphocytic leukemia, *DLBCL* diffuse large B-cell lymphoma, *ECOG* Eastern Cooperative Oncology Group, *FL* follicular lymphoma, *HL* Hodgkin lymphoma, *LOCF* last observation carried forward, *MCL* mantle cell lymphoma, *MDS* myelodysplastic syndromes, *MM* multiple myeloma, *MZL* marginal zone lymphoma, *N* number of subjects, *n* number of observations, *NA* not applicable, *NHL* non-Hodgkin lymphoma, *PD-L1* programmed cell death ligand 1, *SLL* small lymphocytic leukemia, *tFL* transformed follicular lymphoma

depicted by malignancy type in Fig. 3 and Fig. 1 of the ESM, and a time-dependent decrease in CL was observed in patients with NHL and MM. The changes in albumin, IgG, sPD-L1, and LDH with time by malignancy type were shown in Fig. 2 of the ESM.

### 3.4 Impact of Covariates on Durvalumab Exposure

Next, the impacts of these significant covariates at baseline on durvalumab exposure were investigated (Fig. 4). Time-varying covariates (albumin, IgG, sPD-L1, and LDH) were

**Table 3** Population-pharmacokinetic parameter estimates of durvalumab and bootstrap evaluation

Parameter	Parameter estimates (%RSE)	Bootstrap median <sup>a</sup> (95% CI)
<i>Fixed effects</i>		
TVCL, L/h	0.0107 (3.1)	0.0107 (0.0100–0.0113)
TVVc, L	4.63 (2.1)	4.62 (4.43–4.84)
TVQ, L/h	0.0376 (11.6)	0.0375 (0.0298–0.0468)
TVVp, L	2.68 (6.3)	2.69 (2.43–2.98)
ALB on CL <sup>b</sup>	−1.58 (7.1)	−1.58 (−1.81 to −1.36)
IgG on CL <sup>b</sup>	0.258 (12.0)	0.258 (0.193–0.317)
sPD-L1 on CL <sup>b</sup>	0.0617 (37.1)	0.0597 (0.0198–0.116)
LDH on CL <sup>b</sup>	0.115 (33.2)	0.117 (0.0423–0.199)
WT on CL <sup>b</sup>	0.581 (15.5)	0.581 (0.385–0.766)
Sex on CL <sup>b</sup>	0.791 (4.2)	0.789 (0.724–0.857)
MDS/AML on CL <sup>b</sup>	1.26 (4.0)	1.26 (1.15–1.37)
ALB on Vc <sup>c</sup>	−0.566 (18.8)	−0.561 (−0.800 to −0.363)
WT on Vc <sup>c</sup>	0.451 (18.9)	0.448 (0.284–0.591)
Sex on Vc <sup>c</sup>	0.790 (4.2)	0.790 (0.726–0.859)
MM on Vc <sup>c</sup>	0.820 (4.3)	0.822 (0.756–0.893)
<i>Random effects</i>		
Inter-individual variability		
CL, CV%	25.8 (7.9)	25.3 (21.6–29.5)
Vc, CV%	24.7 (5.2)	24.5 (22.1–26.8)
Residual variability		
Log additive error	0.198 (4.3)	0.197 (0.179–0.215)

ALB serum albumin, AML acute myeloid leukemia, CI confidence interval, CL clearance, CV coefficient of variation, IgG immunoglobulin G, LDH lactate dehydrogenase, MDS myelodysplastic syndromes, MM multiple myeloma, Q inter-compartmental clearance, RSE relative standard error, sPD-L1 soluble programmed cell death ligand 1, TV typical value, Vc volume of distribution of central compartment, Vp volume of distribution of peripheral compartment, WT weight

<sup>a</sup>Calculated from 914 bootstraps with successful minimization (out of 1000 bootstraps)

<sup>b</sup>CL (L/h) = 0.0107 × (ALB/40)<sup>−1.58</sup> × (IgG/7.61)<sup>0.258</sup> × (sPD-L1/173.8)<sup>0.0617</sup> × (LDH/216)<sup>0.115</sup> × (WT/74.7)<sup>0.581</sup> × 0.791 (if female) × 1.26 (if MDS/AML)

<sup>c</sup>Vc (L) = 4.63 × (ALB/40)<sup>−0.566</sup> × (WT/74.7)<sup>0.451</sup> × 0.790 (if female) × 0.820 (if MM)

highly variable at baseline and became less variable over time in this study (Fig. 2 of the ESM), suggesting that the greatest impact of these variables should be observed at cycle 1. Therefore, AUC<sub>CL</sub> was used as a typical exposure measure. Significant covariates at baseline were summarized in Fig. 3 of the ESM. Female patients showed a 27% increase in AUC<sub>CL</sub> compared with male patients. Patients with higher albumin (third tertile) and lower albumin (first tertile) had 14% higher and 14% lower AUC<sub>CL</sub> than the second tertile group, respectively. Patients with higher IgG (third tertile) and lower IgG (first tertile) had 14% lower and 16% higher AUC<sub>CL</sub> than the second tertile group, respectively. Patients with higher body weight (third tertile) and lower body weight (first tertile) had 13% lower and 14% higher AUC<sub>CL</sub> than the second tertile group, respectively. For other covariates, the impact on the AUC<sub>CL</sub> (median and 90% CI) was within a 20% increase/decrease. Simulation results demonstrated that both a fixed dose (1500 mg) and a weight-based dose (20 mg/kg) provide a similar durvalumab PK profile in cycle 1 (Fig. 4 of the ESM).

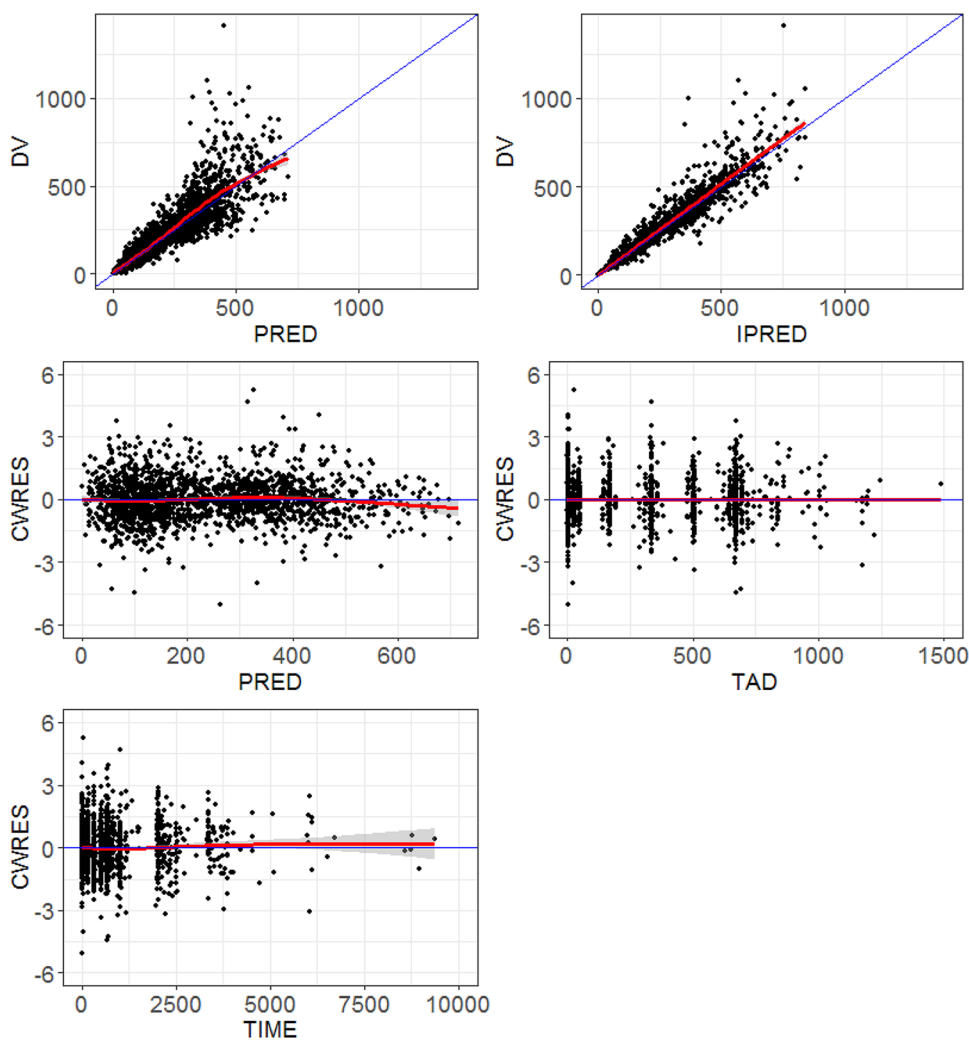
The relationship between albumin and IgG at baseline was explored (Fig. 5a). Interestingly, albumin was positively correlated with IgG up to 20 g/L, which is the upper limit of normal range of IgG, while albumin was negatively correlated with IgG over 20 g/L. Most patients with IgG > 20 g/L were those with MM. The impact of albumin on durvalumab CL was different at IgG of below and above 20 g/L (Fig. 5b). Furthermore, the impacts of subtypes of MM and NHL on durvalumab exposure were evaluated. For MM, patients with IgG of ≥ 20 g/L showed 30% lower AUC compared with patients with IgG of < 20 g/L (Fig. 6a). For NHL, no apparent difference in durvalumab exposure was observed among different subtypes (Fig. 6b).

## 4 Discussion

This is the first study to report a population-PK model of anti-PD-1/PL-1 antibodies in subjects with common hematologic malignancies such as NHL, MM, MDS, and AML. In this population-PK model, durvalumab pharmacokinetics was well described by a two-compartment model with first-order CL. Serum albumin, IgG, sPD-L1, LDH, weight, sex, and some malignancy type (MDS/AML and MM) were incorporated in the final model as covariates on CL and Vc. Change in albumin (in all patients) and IgG (in patients with MM) over time adequately accounts for the time-dependent decrease in durvalumab CL. For MM, patients with IgG of ≥ 20 g/L showed 30% lower AUC compared with patients with IgG of < 20 g/L.

The population-PK model of durvalumab in hematologic malignancies was generally consistent with that in solid tumors [7]. The structural model of durvalumab in this

**Fig. 1** Goodness-of-fit plots of the final population-pharmacokinetic model of durvalumab in subjects with hematologic malignancies. *CWRES* conditional weighted residuals, *DV* observed value, *IPRED* individual predicted values, *PRED* predicted values, *TAD* time after last dose (hour), *TIME* time after first dose (hour). The *blue line* represents the identity line or zero line. The *red line* represents the locally weighted scatterplot smoothing line



analysis was a two-compartment model with first-order CL, which is the most common base model of monoclonal antibodies [13] including other PD-1/PD-L1 inhibitors [4]. Most of the covariates in the final model (albumin on CL, sex on CL and  $V_c$ , and weight on CL and  $V_c$ ) were also observed in the population-PK model of durvalumab in solid tumors [7]. The sPD-L1 level was a covariate on CL and  $V_{max}$  in hematologic and solid tumors, respectively, and a high sPD-L1 level was associated with higher total CL in both models. Additionally, a time-dependent change in albumin significantly improved the fitting of both models.

Several differences were observed in the base model structure between the two durvalumab population-PK models in patients with hematologic malignancies and solid tumors. Nonlinear CL was not included in our population-PK model of durvalumab in hematologic malignancies, while a previous population-PK model of durvalumab in solid tumors contained nonlinear Michaelis–Menten CL [7]. In addition, we failed to obtain robust parameter estimates of the empirical time-varying CL model. The

discrepancy in nonlinearity may in part be explained by the difference in dose levels of durvalumab. Durvalumab showed nonlinear pharmacokinetics with saturable target-mediated CL at doses < 3 mg/kg, and the solid tumor model included data from doses ranging from 0.1 to 20 mg/kg [7]. However, our four clinical trials in subjects with hematologic malignancies tested only one dose and at a relatively high dose level, 1500 mg every 4 weeks (equivalent to 10 mg/kg every 2 weeks or 20 mg/kg every 4 weeks), where the linearity of exposure with doses was approached. Failure to add the empirical time-varying CL model into the current model could be explained in part by the shorter follow-up period of PK sampling. In the previously reported durvalumab model [7], population mean value of  $T_{50}$  was 173 days (about 5 months). In our analysis, 85% and 95% of concentrations were obtained within 2 and 4 months after the first dose, indicating the difficulty of estimating robust empirical time-varying CL model parameters in our model. The goodness-of-fit plot (conditional weighted residual vs. time after first dose,

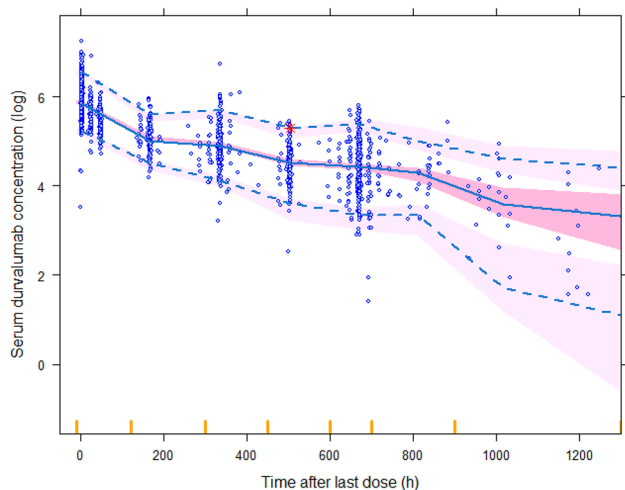


**Fig. 2** Visual predictive check for durvalumab in subjects with hematologic malignancies. Circles represent observed data. Lines represent the 5th (dashed), 50th (solid), and 95th (dashed) percentiles of the observed data. Shaded areas represent nonparametric 90% confidence intervals about the 5th (light pink), 50th (dark pink), and 95th (light pink) percentiles for the corresponding model-predicted percentiles

Fig. 1) of the final model did not show any under-prediction of durvalumab concentrations at later timepoints, justifying the final model with time-varying covariates.

The covariate with the largest impact on durvalumab exposure was sex, and female patients showed 27% higher exposure than male patients (Fig. 4). In the final population-PK model, lower body weight and being female were independently associated with lower durvalumab CL, which is often observed in other monoclonal antibodies [13]. In this study, median body weight of female patients (63.5 kg) was 20% lower than that of male patients (79.0 kg). Effect of sex on durvalumab exposure was higher in hematologic malignancies (27%) compared with solid tumors (17%) [7], which would be in part owing to larger actual doses in female patients in studies of hematologic malignancies, caused by the switch from a weight-based dosing regimen in solid tumor studies (10 mg/kg every 2 weeks) to a fixed dosing regimen in hematologic malignancy studies (1500 mg every 4 weeks). Simulation results indicated the similar durvalumab concentration–time profile between 1500 mg and 20 mg/kg (which is comparable to 1500 mg). The slightly higher 95 percentile concentration in 1500 mg would be explained by the larger actual dose in female patients. Nevertheless, the impact of sex on durvalumab pharmacokinetics would not be clinically significant because the impact of sex was relatively small and no exposure–efficacy or exposure–safety relationship for durvalumab was observed in patients with solid tumors receiving the recommended dosing regimen (10 mg/kg every 2 weeks) [14]. Overall, the

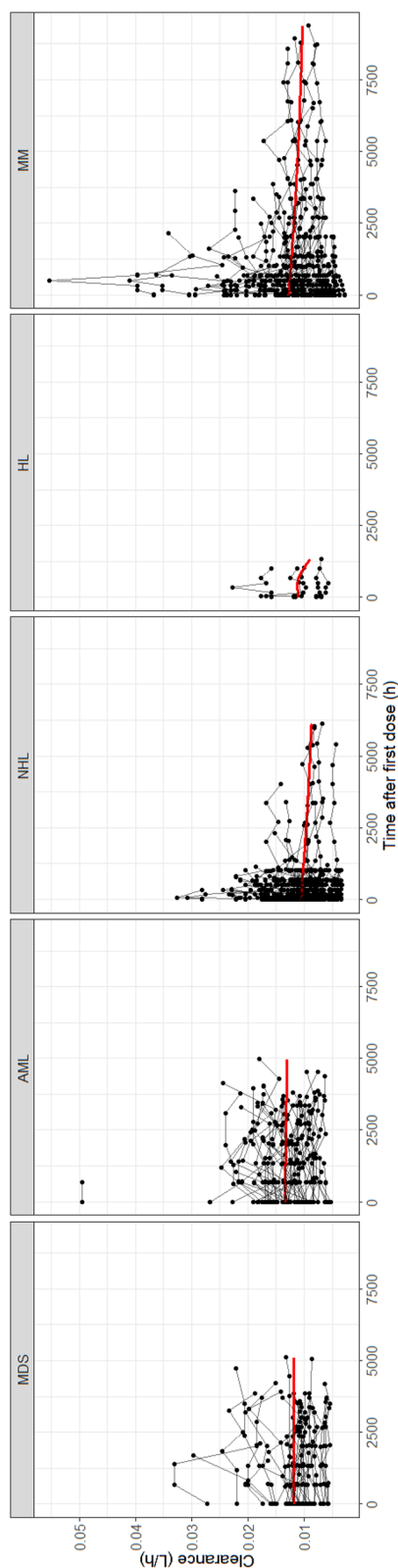


**Fig. 3** Time-dependent clearance of durvalumab by type of hematologic malignancy. The red line represents the locally weighted scatterplot smoothing line. *AML*, acute myeloid leukemia, *CL* clearance, *HL* Hodgkin lymphoma, *MDS* myelodysplastic syndromes, *MM* multiple myeloma, *N* number of subjects, *NHL* non-Hodgkin lymphoma



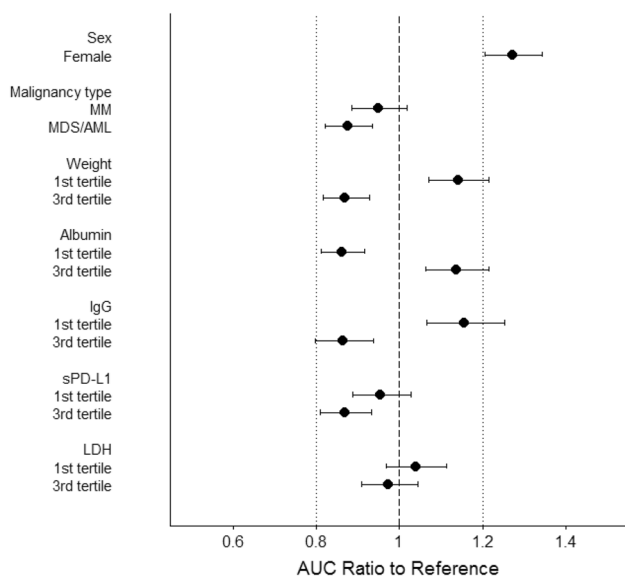


**Fig. 4** Forest plot of baseline covariates on durvalumab exposure. Data are shown as median (90% confidence interval). References are male (sex), non-Hodgkin lymphoma, and Hodgkin lymphoma (malignancy type) and second tertile (weight, albumin, immunoglobulin G [IgG], soluble programmed cell death ligand 1 [sPD-L1] and lactate dehydrogenase [LDH]). First, second, and third tertile of weight at baseline are 37.7–68.5 kg, 68.6–80.1 kg, and 80.5–121 kg, respectively. First, second, and third tertile of albumin at baseline are 23–38 g/L, 39–42 g/L, and 43–50 g/L, respectively. First, second and third tertile of IgG at baseline are 0.70–4.99 g/L, 5.00–10.4 g/L, and 10.5–73.7 g/L, respectively. First, second, and third tertile of sPD-L1 at baseline are 72.0–145.5 pg/mL, 145.7–204.1 pg/mL, and 204.5–984.6 pg/mL, respectively. First, second, and third tertile of LDH at baseline are 89–190 U/L, 191–261 U/L, and 263–1481 U/L, respectively. Area under the concentration–time curve at cycle 1 (AUC) of durvalumab was used as an exposure parameter and calculated based on individual Bayesian estimates of PK parameters at baseline from the final population-PK model

impact of any baseline covariates on durvalumab pharmacokinetics did not appear to be clinically meaningful.

Incorporation of albumin and IgG as time-varying covariates in the final model significantly improved the statistical fit ( $\Delta$ OFV:  $-239$  and  $-153$ , respectively). An apparent time-dependent increase in albumin and a decrease in IgG were observed in patients with NHL and MM, respectively (Fig. 2 of the ESM). In the time-invariant model, baseline albumin and IgG reduced OFV by 35 and 62, respectively (data not shown), indicating the appropriateness of time-varying covariates in the final model. Soluble PD-L1 improved the statistical fit as a time-varying covariate ( $\Delta$ OFV:  $-18$ ), however, it was not retained in the final time-invariant model (data not shown). The sPD-L1 level in most patients with available sPD-L1 data at a later time was lower than the limit of detection (Fig. 2 of the ESM), accounting for a 16% decrease in CL from the baseline at cycle 2 and beyond. The decrease in OFV by including time-varying LDH was 15,

which was comparable to that of the time-invariant model ( $\Delta$ OFV:  $-27$ , data not shown), indicating the impact on CL would be mostly accounted for by the LDH at baseline. As shown in Fig. 4, the effect of LDH on durvalumab exposure was minimal.

The neonatal Fc receptor plays a critical role in salvaging both IgG and albumin from lysosomal degradation [15]. Albumin level was positively correlated with IgG at below 20 g/L of IgG, which is the upper range of normal IgG levels (Fig. 5a). This suggests that at normal IgG levels, a lower albumin level could be an indicator of higher CL of both albumin and IgG (including externally administered monoclonal antibodies) [13]. However, the albumin level decreased with an increasing IgG level above 20 g/L (Fig. 5a), where the salvage of IgG and albumin by the neonatal Fc receptor appeared to be saturated. Hypergammaglobulinemia is commonly seen in patients with MM, and the higher CL of monoclonal antibodies in this populations has been suggested [16, 17]. The current study demonstrated that albumin and IgG were independent covariates of the durvalumab population-PK model and the impact of albumin on durvalumab CL was different at IgG of below and above 20 g/L (Fig. 5b). These findings suggest that both albumin and IgG are independent determinants of CL of monoclonal antibodies in patients with MM with hypergammaglobulinemia, while albumin could be enough to explain the CL of monoclonal antibodies at the normal range of IgG levels. A time-dependent decrease in durvalumab CL would be explained by the change in IgG over time in patients with MM, which is consistent with a time-dependent decrease in CL of daratumumab in patients with MM [18].

The type of hematologic malignancy had a relatively small impact on durvalumab pharmacokinetics. The differences in durvalumab exposure (median and 90% CI) were within 20% among MDS/AML, MM, and NHL/Hodgkin lymphoma (Fig. 4). In addition, there was no apparent difference in durvalumab exposure among various NHL subtypes (Fig. 6b). For MM, hypergammaglobulinemia was a key determinant of durvalumab exposure (Fig. 6a).

Our study was limited by a single-dose level and a relatively shorter collection duration of PK data. Because only one dose level of durvalumab (1500 mg every 4 weeks) was included in this population-PK analysis, it is difficult to capture nonlinear CL of durvalumab that was observed over a wide dose range in solid tumors [7]. In addition, the PK sampling period from the first dose in our analysis was shorter than that in the previous analyses of durvalumab and other PD-1/PD-L1 inhibitors where empirical time-varying CL was implemented [7–9]. Therefore, we could not draw an unequivocal conclusion that these differences between the current and previous analyses is due to the difference in tumor type (solid tumors vs. hematologic malignancies). Rather, durvalumab pharmacokinetics in

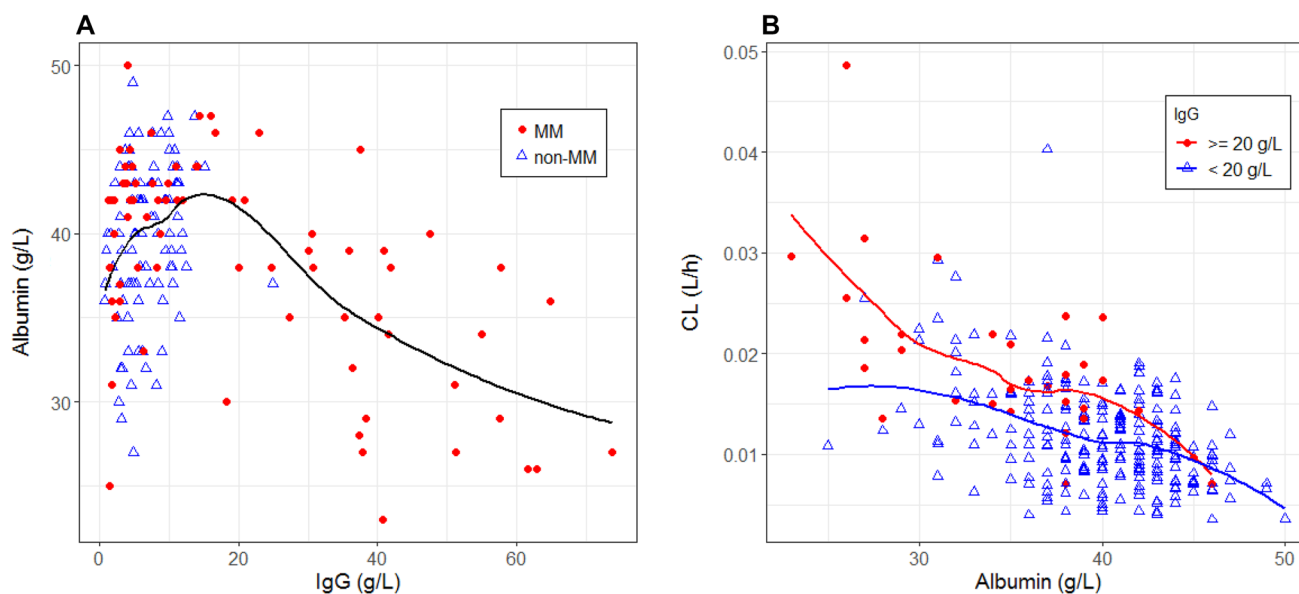


**Fig. 5** Association of albumin with immunoglobulin G [IgG] (a) and durvalumab clearance (CL) controlling IgG (b). The lines represent the locally weighted scatterplot smoothing lines. *MM* multiple myeloma

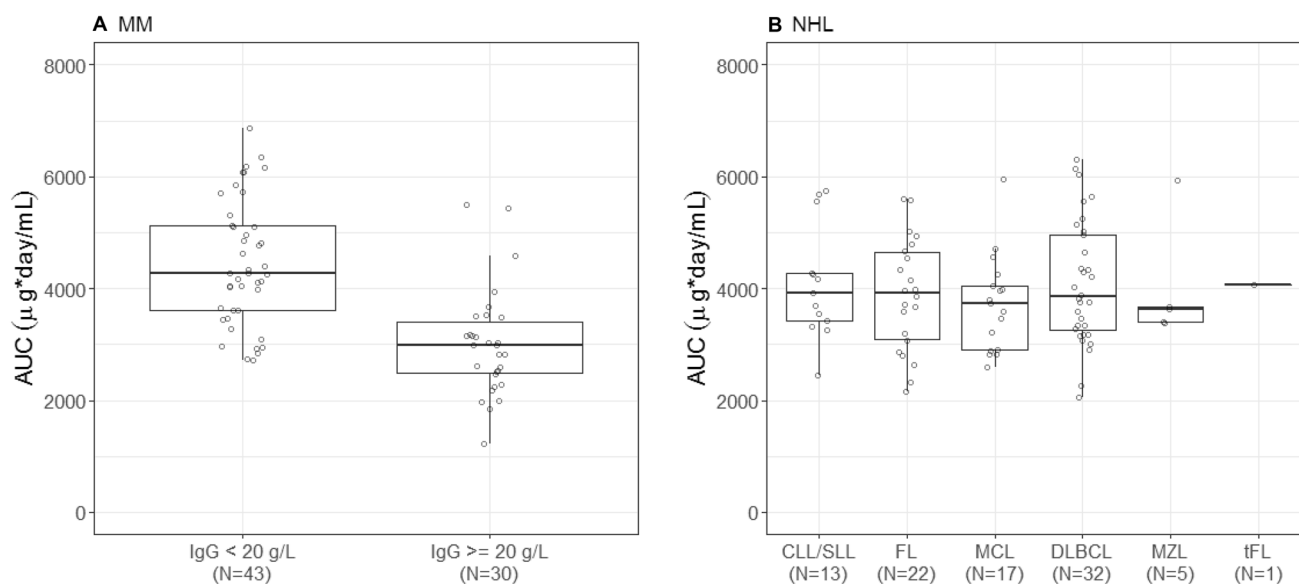


**Fig. 6** Effects of hypergammaglobulinemia in multiple myeloma [MM] (a) and subtype of non-Hodgkin lymphoma [NHL] (b) on durvalumab exposure. *AUC* area under the concentration–time curve at cycle 1, *CLL* chronic lymphocytic leukemia, *DLBCL* diffuse large

B-cell lymphoma, *FL* follicular lymphoma, *IgG* immunoglobulin G, *MCL* mantle cell lymphoma, *MZL* marginal zone lymphoma, *N* number of subjects, *SLL* small lymphocytic leukemia, *tFL* transformed follicular lymphoma

hematologic malignancies was mostly consistent with that in solid tumors. Second, some time-varying covariates were not available from all patients (IgG) or available at less frequent timepoints (sPD-L1). Time-varying IgG data were available only from patients with MM. More complete time-varying data of IgG and sPD-L1 would improve the statistical fit of the population-PK model; however, the impact would be

minimal because of the following reasons: (1) sPD-L1 level is considered to affect nonlinear CL; however, the contribution of nonlinear CL to the total CL of durvalumab is small and (2) hypergammaglobulinemia in non-MM hematologic malignancies is not as common as MM, and a significant time-dependent change in IgG is not expected in non-MM hematologic malignancies.

## 5 Conclusions

The pharmacokinetics of durvalumab in hematologic malignancies was generally consistent with that in solid tumors, and these results support the same dosing regimen (1500 mg every 4 weeks) for both solid tumors and hematologic malignancies. In addition, IgG level was indicated to be a critical covariate of monoclonal antibodies in patients with MM.

**Acknowledgments** The authors thank all study participants and their families. We also thank the clinical study team members at the study sites, Celgene Corporation and the contract research organizations.

## Compliance with Ethical Standards

**Funding** This study was funded by Celgene Corporation.

**Conflict of Interest** Ken Ogasawara, Kathryn Newhall, Stephen E. Maxwell, Justine Dell'Aringa, Vitalina Komashko, Nurgul Kilavuz, Richard Delarue, Myron Czuczman, Lars Sternas, Shelonitda Rose, C.L. Beach, Steven Novick, Simon Zhou, Maria Palmisano, and Yan Li are employees of Celgene Corporation and hold equity ownership in Celgene Corporation.

**Ethics Approval** All procedures performed in the studies involving human participants were in accordance with the ethical standards of the institutional and/or national research committee and with the 1964 Helsinki Declaration and its later amendments or comparable ethical standards.

**Consent to Participate** Informed consent was obtained from all individual participants included in the study.

**Open Access** This article is distributed under the terms of the Creative Commons Attribution-NonCommercial 4.0 International License (<http://creativecommons.org/licenses/by-nc/4.0/>), which permits any noncommercial use, distribution, and reproduction in any medium, provided you give appropriate credit to the original author(s) and the source, provide a link to the Creative Commons license, and indicate if changes were made.

## References

- Chen L, Han X. Anti-PD-1/PD-L1 therapy of human cancer: past, present, and future. *J Clin Invest*. 2015;125(9):3384–91. <https://doi.org/10.1172/JCI80011>.
- Stewart R, Morrow M, Hammond SA, Mulgrew K, Marcus D, Poon E, et al. Identification and characterization of MEDI4736, an antagonistic anti-PD-L1 monoclonal antibody. *Cancer Immunol Res*. 2015;3(9):1052–62. <https://doi.org/10.1158/2326-6066.CIR-14-0191>.
- US Food and Drug Administration. Drugs@FDA: FDA approved drug products. <https://www.accessdata.fda.gov/scripts/cder/daf/>. Accessed 11 Feb 2019.
- Sheng J, Srivastava S, Sanghavi K, Lu Z, Schmidt BJ, Bello A, et al. Clinical pharmacology considerations for the development of immune checkpoint inhibitors. *J Clin Pharmacol*. 2017;57(Suppl. 10):S26–42. <https://doi.org/10.1002/jcph.990>.
- Ahamadi M, Freshwater T, Prohn M, Li CH, de Alwis DP, de Greef R, et al. Model-based characterization of the pharmacokinetics of pembrolizumab: a humanized anti-PD-1 monoclonal antibody in advanced solid tumors. *CPT Pharmacometrics Syst Pharmacol*. 2017;6(1):49–57. <https://doi.org/10.1002/psp4.12139>.
- Bajaj G, Wang X, Agrawal S, Gupta M, Roy A, Feng Y. Model-based population pharmacokinetic analysis of nivolumab in patients with solid tumors. *CPT Pharmacometrics Syst Pharmacol*. 2017;6(1):58–66. <https://doi.org/10.1002/psp4.12143>.
- Baverel PG, Dubois VFS, Jin CY, Zheng Y, Song X, Jin X, et al. Population pharmacokinetics of durvalumab in cancer patients and association with longitudinal biomarkers of disease status. *Clin Pharmacol Ther*. 2018;103(4):631–42. <https://doi.org/10.1002/cpt.982>.
- Li H, Yu J, Liu C, Liu J, Subramaniam S, Zhao H, et al. Time dependent pharmacokinetics of pembrolizumab in patients with solid tumor and its correlation with best overall response. *J Pharmacokinetic Pharmacodyn*. 2017;44(5):403–14. <https://doi.org/10.1007/s10928-017-9528-y>.
- Liu C, Yu J, Li H, Liu J, Xu Y, Song P, et al. Association of time-varying clearance of nivolumab with disease dynamics and its implications on exposure response analysis. *Clin Pharmacol Ther*. 2017;101(5):657–66. <https://doi.org/10.1002/cpt.656>.
- Stroh M, Winter H, Marchand M, Claret L, Eppler S, Ruppel J, et al. Clinical pharmacokinetics and pharmacodynamics of atezolizumab in metastatic urothelial carcinoma. *Clin Pharmacol Ther*. 2017;102(2):305–12. <https://doi.org/10.1002/cpt.587>.
- Wilkins JJ, Brockhaus B, Dai H, Vugmeyster Y, White JT, Brar S et al. Time-varying clearance and impact of disease state on the pharmacokinetics of avelumab in merkel cell carcinoma and urothelial carcinoma. *CPT Pharmacometrics Syst Pharmacol*. 2019. <https://doi.org/10.1002/psp4.12406>.
- Wang X, Ludwig EA, Passarelli J, Bello A, Roy A, Hruska MW. Population pharmacokinetics and exposure-safety analyses of nivolumab in patients with relapsed or refractory classical Hodgkin lymphoma. *J Clin Pharmacol*. 2019;59(3):364–73. <https://doi.org/10.1002/jcph.1324>.
- Ogasawara K, Alexander GC. Use of population pharmacokinetic analyses among FDA-approved biologics. *Clin Pharmacol Drug Dev*. 2019. <https://doi.org/10.1002/cpdd.658>.
- Jin CY, Zheng Y, Jin X, Mukhopadhyay P, Gupta A, Dennis PA, et al. Exposure-efficacy and safety analysis of durvalumab in patients with urothelial carcinoma (UC) and other solid tumors. *J Clin Oncol*. 2017;35(15):2568.
- Pyzik M, Rath T, Lencer WI, Baker K, Blumberg RS. FcRn: the architect behind the immune and nonimmune functions of IgG and albumin. *J Immunol*. 2015;194(10):4595–603. <https://doi.org/10.4049/jimmunol.1403014>.
- Jacobs JFM, Mould DR. The role of FcRn in the pharmacokinetics of biologics in patients with multiple myeloma. *Clin Pharmacol Ther*. 2017;102(6):903–4. <https://doi.org/10.1002/cpt.665>.
- Xu XS, Schecter JM, Jansson R, Yan X. Response to “The role of FcRn in the pharmacokinetics of biologics in patients with multiple myeloma”. *Clin Pharmacol Ther*. 2017;102(6):905. <https://doi.org/10.1002/cpt.779>.
- Xu XS, Yan X, Puchalski T, Lonial S, Lokhorst HM, Voorhees PM, et al. Clinical implications of complex pharmacokinetics for daratumumab dose regimen in patients with relapsed/refractory multiple myeloma. *Clin Pharmacol Ther*. 2017;101(6):721–4. <https://doi.org/10.1002/cpt.577>.